International Journal of Recent Technology and Engineering (IJRTE)
ISSN: 2277-3878, Volume-8 Issue-3, September 2019

Classification of Land Cover from Remote Sensing Images using Morphological Linear Contact Distributions and Rough Sets.

A.V. Kavitha, A. Srikrishna, Ch. Satyanarayana

Abstract*: Remote sensing image classification plays an essential role in computer vision and image processing to address the problems in the areas of agriculture, forest monitoring, urban development, environment protection, etc. A lot of literature is available on remote sensing image classification. But, it is still a research task even today because of the multitude of problems. RTBFCA (Rough Texture Based Features Classification Algorithm), a new classification algorithm has been proposed in this paper. This paper aims at classifying the remote sensing images into various cover types using mathematical morphology and rough sets. Morphological texture features (linear contact distributions) along with first order statistics are used to identify the pixels of various classes and the concepts of lower and upper approximations of rough sets are used for clustering the features of the pixels and then are finally classified to display the classified image. The proposed method was tested on Google Earth images and is able to classify even various crops patterns of a land cover image. The algorithm is compared with other algorithms like "GLCM with rough sets", "intensity values with rough sets" and with "linear contact distributions with rough sets".

Keywords* : *Remote sensing images, mathematical morphology, rough sets, linear contact distributions, classification.

I. INTRODUCTION

From the inception of remote sensing images, remote sensing image segmentation or classification has been considered to be one of the significant tasks. Considerable efforts are made to classify land use and land cover satellite data to help in the classification of crops[9], forest strands[16], rivers [19], snow cover, traditional land use and land cover classification[6], [37], [31], oil spills in the ocean[28], roads[22], sand ridges, etc. However remotely sensed image classification is a challenging task even today, due to the multitude of the complications. For example, any two regions of the same class as per ground truth may appear different in the remote sensing image due to weather conditions, the timing of the image acquired, different sensors used, etc.

A significant portion of work has been reported in the literature on feature extraction for classification of a remotely sensed image [31], [23], [29]. Most of them are based on either pixel, texture or shape information. But, classifying a pixel depending on its own information may not be sufficient as spatial content among pixels is ignored. In this context, using texture information might be a better choice as the information in remote sensing images is also highly textured. Number of approaches like gray scale co-occurrence matrices [26], [27], Markov random field, wavelets [14], [3], watershed [34], [20] algorithms etc are proposed for extracting texture features from an image. Most of them are tested on artificial textures. Textures of remote sensing images are more challenging as they are natural textures. Several approaches are proposed in literature where remote sensing images are classified with texture features [29], [26], [7], [27], [3]. After acquiring the features of every pixel, all the pixels of the image are to be clustered to classify the image. If simple k-means is used for clustering, the object must be assigned to only one cluster at a time. In order to deal with the ambiguity and uncertainty in clustering, nowadays rough sets theory is gaining more attention [38]. Lingras and West used rough sets for web mining [21]. Ying Wang, Xiaoyun Liu, et al have used rough sets for reducing the multispectral bands in a multi spectral remote sensing image using the concept of reduct in rough sets [35]. Rudra Kalyan Naik, Debahuti Mishra, et al used rough sets for clustering and pattern recognition in leukemia data set [24]. Anupama, et al have used rough sets for classification of medical images [1], [2]. But most of them used intrinsic values for classification. Though few algorithms have been proposed for remotely sensed image classification [15], [35], [36], [40], [39], they either used decision rules, optimization algorithms or neural networks along with rough sets.

In this paper, we propose an unsupervised algorithm RTBFCA to classify remotely sensed images acquired from Google Earth into various cover types using morphological texture features, first order statistics and the concepts of lower and upper bound approximations of rough sets. RTBFCA has been compared with other algorithms like "intensity values with rough sets", "GLCM with rough sets", and with "linear contact distributions with rough sets" and obtained promising results.

Manuscript published on 30 September 2019
* Correspondence Author
A.V.Kavitha*, Associate professor, Sri. A.B.R. Govt. degree college, Repallle, Guntur(Dt), Andhra Pradesh, India and Research scholar, Jawaharlal Nehru technological university – Kakinada, Kakinada, Andhra Pradesh, India. Email: anubrolukavitha@yahoo.com
Dr. A. Srikrishna, Professor and HOD, Department of Information and Technology, RVR JC College of engineering, Chowdavaram, Guntur, Andhra Pradesh, India. Email: atlurisrikrishna@yahoo.com
Dr. Ch. Satyanarayana, Professor, Department of computer science, Jawaharlal Nehru technological university - Kakinada, Kakinada, Andhra Pradesh, India.department, Name of the affiliated College or University/Industry, City, Country. Email: chsatyanarayana@yahoo.com

The organization of the paper is as follows. Section 2 presents the background, section 3 explains the proposed methodology, Experimental setup has been explained in Section 4, Results and discussions along with comparison of RTBFCA with other algorithms have been presented in Section 5 and finally, conclusion has been presented in section 6.

II. BACKGROUND

A. Linear contact distributions (LCD)

Mathematical morphological texture features used in this paper are linear contact distributions which have been proposed in [12], where promising results have been obtained. Every binary image can be represented as a random closed set. To get the feature vector of a pixel, linear contact distributions of that pixel in four principal directions are calculated [11]. If 'W' is the array of pixels and 'N' is the set of pixels with value '1' and if "$\varepsilon_Y(X)$" represents erosion of set 'X' by set 'Y', then the linear contact distribution for a line segment 'K' with an angle '$\propto$' can be estimated with the following equation.

$$H^{\alpha}(K) = 1 - \frac{A(\varepsilon_{s(k,\alpha)}(N)^c).A(W)}{A(\varepsilon_{s(k,\alpha)}(W)).A((N)^c)} \qquad (1)$$

Where S(k, $\propto$) is a structuring element, which represents a line segment having length 'K' and angle $\propto$. Here angle $\propto$ = 0^o, 45^o, 90^o,135^o are considered. 'A' is understood as area, here calculated as the number of pixels [11].

B. Rough Sets

To handle imprecise and uncertain knowledge, rough set theory [38] was introduced. Let 'U' be the Universe, and 'R' is the indiscernible relation, such that R $\subseteq$ U x U. Here 'R' represents imprecise or vague elements of 'U'. Also, assume 'X' is the subset of 'U'. Now, the rough set 'R' is given by < $\overline{R}(X)$, $\underline{R}(X)$ > [38]

Where

$$\underline{R} = \bigcup_{x_i \in X} X \qquad (2)$$

and

$$\overline{R} = \bigcup_{x_i \cap X \neq 0} X \qquad (3)$$

$\underline{R}(X)$ represents the lower approximation space of "X". Lower approximation of a set 'X' with respect to 'R' is the set of all elements that definitely belongs to 'X'. $\overline{R}(X)$ represents the upper approximation space of 'X'. Upper approximation of set 'X' with respect to 'R' is the set of all elements that can be possibly classified as 'X'. The boundary region of 'X' with respect to 'R' is the set of all elements which can neither be classified as 'X' nor as "not X" with respect to 'R'. Set 'X' is crisp [38], [24] if boundary region of 'X' is empty and set 'X' is rough, if the boundary region of 'X' is not empty.

C. First Order Statistics (FOS)

Employing statistics for texture analysis is one of the early, simple and traditional methods. First order, second order and third order statistical texture measures can be used for texture feature extraction from an image [32]. First order statistical measures use only the intensity values of the individual pixels present in the image. Spatial relationships with the neighbouring pixels are not considered in first-order statistics texture methods. Second order statistics use two pixels, third order statistics use three pixels and so on to estimate the features based on the properties of the pixel values relative to each other [32], [33]. Mean, variance, first order moments, second-order moments, etc are a few examples of first-order statistical texture measures.

D. Gray Level Co-occurrence Matrix (GLCM)

Gray level co-occurrence matrix has been proposed by Harlick et al [17], which used second order statistical measures and could be used to estimate the texture properties of an image. GLCM has been used in various applications [26], [27], [33]. It is expressed in the form of a matrix and represents the frequency of various combinations of gray values occurs in the image. If 'G' is the number of gray level values present in the image, then 'G' number of rows and 'G' number of columns are present in the gray level co-occurrence matrix. Every matrix element of GLCM p(i,j / d, ɵ) is the estimation value of the frequency with which the two pixels having intensity values 'i' and 'j' with 'd' distance and 'ɵ' angle present in the image. Based on these values of GLCM, Harlick et al have proposed 14 texture estimation measures like contrast, correlation, angular second moment, etc[17].

III. PROPOSED METHODOLOGY

Before Considering binary image as a random closed set, Irene Epifanio and Guillermo Ayala have proposed extracting texture features of every pixel with linear contact distributions [12]. But, they have applied them on artificial texture. As remote sensing images are natural, they are more complicated to classify. Later Irene Epifanio and Pierre Soille have used linear contact distributions to estimate the texture features from remote sensing images [11]. Both supervised and unsupervised algorithms are proposed by them to classify remote sensing images. But, in the unsupervised algorithm, a tedious procedure of rotating and moving windows is employed to classify the texture features. Hence in the proposed algorithm RTBFCA, a new method to extract the features with the help of linear contact distributions and to finally classify them with the help of rough sets is proposed for automatic classification of a remote sensing image. The flow of the whole algorithm is explained as follows.

A gray scale image 'G' has been obtained from the given Google Earth remotely sensed image 'I'. From gray scale image 'G', four binary images 'B1', 'B2', 'B3' and 'B4' have been generated, by applying various mathematical transformations.

For every pixel ‘p’, from every binary image, using linear contact distributions four features are extracted. Thus, for every pixel in ‘G’ 16 features are extracted. Using first order statistics, again four more features are extracted for every pixel ‘p’. Thus, for every pixel ’p’ in the given image, a total of twenty features are extracted. Using the concepts of lower and upper bounds of rough sets, the features of the image are clustered. Finally, the classified remotely sensed image is displayed. The proposed methodology has been presented in the flowcharts 1, 2 and 3.

A. Texture feature extraction using linear contact distributions

Initially, two thresholds ‘t1’ and ‘t2’ are estimated from the given gray scale image ’G’ [4]. With the help of these thresholds ‘t1’ and ‘t2’, four binary images are generated from image ‘G’. The following algorithm explains the procedure for the generating binary images.

Algorithm to generate four binary images.

Input: Given image ‘G’.

Output: Four binary images ‘B1’, ‘B2’, ‘B3’ and ‘B4’.

Step 1: Using OTSU method [25], [18], a threshold value ‘th1’ is estimated from the given gray scale image .

Step 2: Multiply ‘th1’ with maximum intensity value 255 to get the first threshold value ‘t1’.

Step 3: The image ‘G’ is converted into a binary image ‘B’ using the threshold value ‘t1’. All values less than or equal to ‘t1’ are considered as ‘1’ and values greater than ‘t1’ are considered as ‘0’, to obtain the binary image ‘B’.

Step 4: Dilate the image ‘G’ with structuring element S = [1,1,1;1,1,1;1,1,1] to get the dilated image ‘DG’.

Step 5: Find the external gradient image ‘E’, by subtracting ‘G’ from ‘E’.

Step 6: Estimate the threshold ‘th2’ for external gradient image ‘E’ using OTSU method.

Step 7: Multiply ‘th2’ with the maximum intensity value 255 to get the second threshold value ‘t2’.

Step 8: External gradient images E1, E2, E3, and E4 are obtained from image ‘G’ using the following structuring elements.

S1 = Square with side ‘11’.

S2 = Diamond with radius ‘7’.

S3 = Disc with radius ‘ 7 ‘ and

S4 = Cross with side ‘5’.

Step 9: Thresholded external gradient images T1, T2, T3, and T4 are generated from gradient images E1, E2, E3 and E4 using the threshold value ‘t2’. All values greater than or equal to ‘t2’ are considered as ‘1’ and remaining as ‘0’ in the output images.

Step 10: Thresholded external gradient images T1, T2, T3, and T4 are intersected with binary image ‘B’ to get the intersected images ‘I1’, ‘I2’, ‘I3’ and ‘I4’.

Step 11: Final binary images ‘B1’, ‘B2’, ‘B3’ and ‘B4’ which are used to extract texture features are obtained by area opening the images ‘I1’, ‘I2’, ‘I3’ and ‘I4’ with value 10.

Step 12: Stop.

For every pixel ‘p’ in each binary image, a window ‘W’ of size 51 x 51 is considered having the pixel ‘p’ in the center. For this window ‘W’, four features are calculated using linear contact distributions with the help of equation 1. A line segment oriented with angles 0 degrees, 45, 90 and 135 is used in equation 1 to get four features for every pixel in every binary image. Thus in total 16 features are extracted for every pixel from four binary images for every pixel [11].

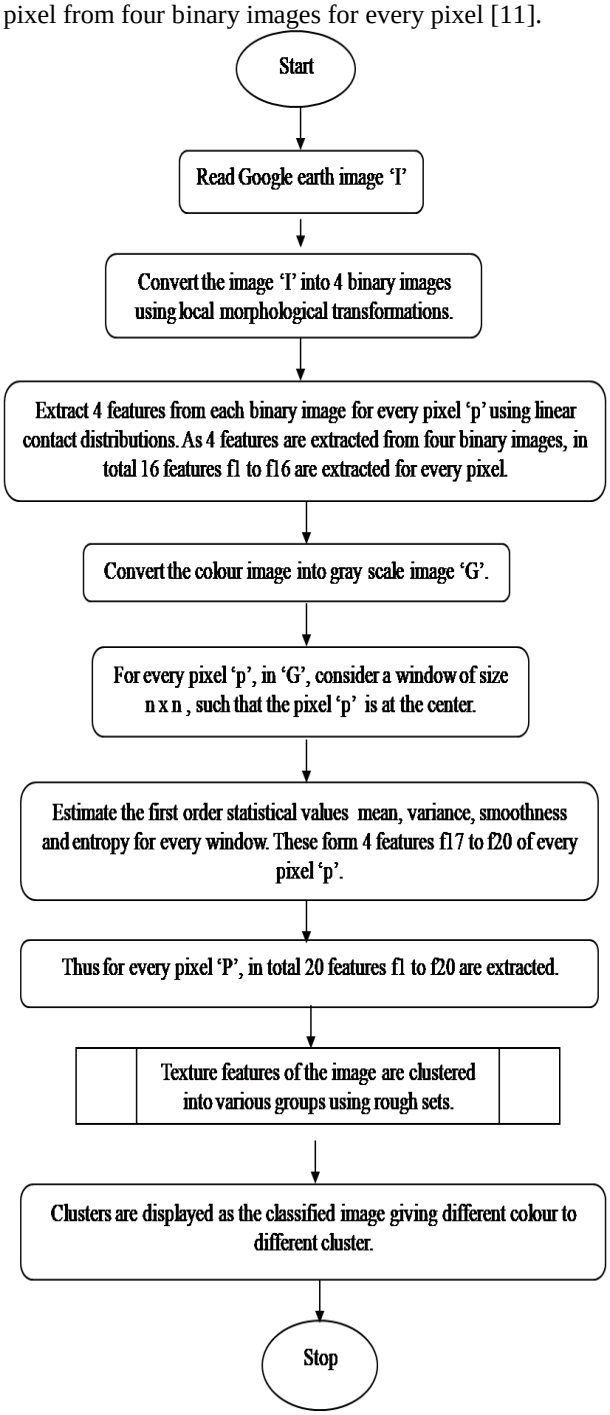

Fig. 1: Flow chart for proposed algorithm RTBFCA

B. Texture feature extraction using first order statistics

For every pixel ‘p’ in the gray scale image ‘G’, a window of size 51 X 51 has been considered around the pixel ‘p’. ‘p’ should be the center pixel of the window. Now calculate four features Mean, Variance, Smoothness index and Entropy of the window [33, 5].

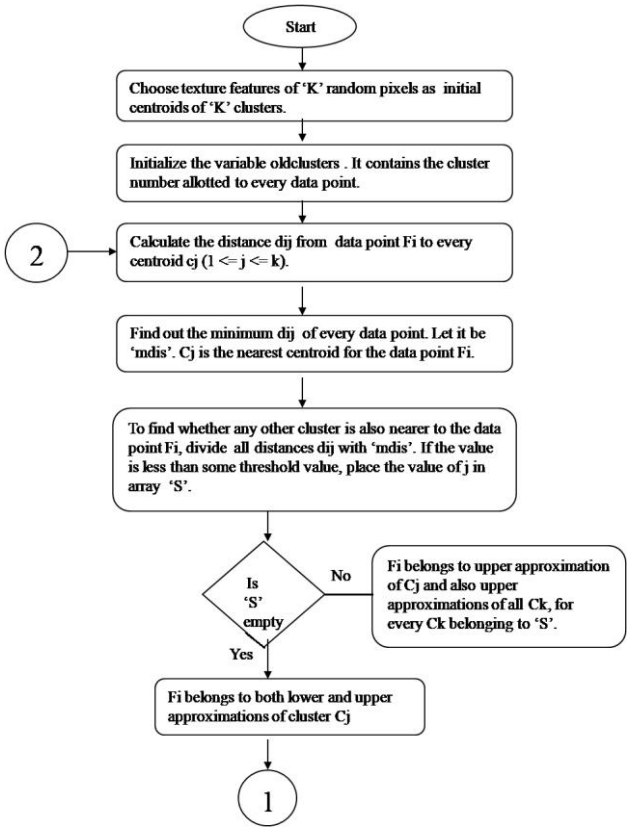

Fig. 2: Flow chart for proposed methodology - subprocess

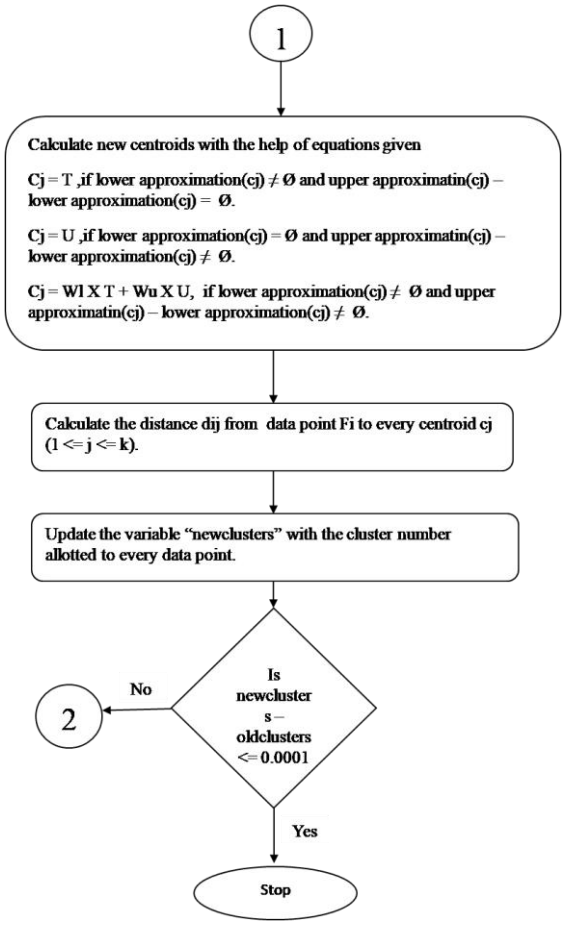

Fig. 3: Flow chart for proposed methodology - subprocess continued

C. Clustering using Rough sets

Four features with the help of first order statistics and 16 features with the help of linear contact distributions are extracted for every pixel in the input image. To handle the ambiguity and uncertainty at the borders of various segments, rough sets are used to cluster the pixels of the image. Similar to the k-means algorithm, centroids are calculated to every cluster in the rough sets clustering algorithm. Initially, feature vectors of some k random pixels are taken as the centroids c1, c2, .. ck for k clusters. Distance of data point (feature vector of the pixel) say Fi to every centroid cj (1 <= j <= k) is calculated. Let dij be the smallest distance. To verify whether any other cluster is also nearer to the data point Fi, divide all the similarity distances with dij. If there are any such values less than some threshold value, that means there could be some other clusters which are also nearer to the data point Fi along with cluster cj. In such cases, data point Fi is allotted to the upper approximations of both the clusters. Otherwise, if there are no values less than the threshold value, that means this feature vector or pixel definitely belongs to only cluster cj. That is why the data point Fi is allotted to the lower approximation of cj and also an upper approximation of cj. After completing calculating the similarity distances of the feature vectors of all pixels and allocating them to the required clusters, the new centroids of all the clusters are calculated with the following formula [21], [1], [24].

$$n_j = \begin{cases} T & \text{if } \underline{R}(c_j) \neq \varnothing \text{ and } \overline{R}(c_j) - \underline{R}(c_j) = \varnothing \\ U & \text{if } \underline{R}(c_j) = \varnothing \text{ and } \overline{R}(c_j) - \underline{R}(c_j) \neq \varnothing \\ V & \text{if } \underline{R}(c_j) \neq \varnothing \text{ and } \overline{R}(c_j) - \underline{R}(c_j) \neq \varnothing \end{cases} \quad (4)$$

Where

$$T = \frac{\sum_{x \in \underline{R}(c_j)} F_i}{\left| \overline{R}(c_j) - \underline{R}(c_j) \right|} \quad (5)$$

$$U = \frac{\sum_{x \in \left(\overline{R}(c_j) - \underline{R}(c_j) \right)} F_i}{\left| \overline{R}(c_j) - \underline{R}(c_j) \right|} \quad (6)$$

$$V = W_l \times T + W_u \times U \quad (7)$$

W_l the weight for lower approximation and Wu is the weight for upper approximation. This process is iterated until there is no significant change in the clusters being formed. The following algorithm explains the clustering process with rough sets.

Algorithm for segmentation using Rough sets:
Input :
Feature vectors Fi of every pixel in the image,
number of clusters K,
old clusters (An array variable to hold cluster value allotted for every pixel in the previous iteration. Size of the array will be mn x 1, where the image is of size m x n.) and
new clusters (An Variable to hold cluster value allotted for every pixel in the present iteration).

Output:
An array 'new clusters' containing cluster number allotted for every pixel (segmented data).

Algorithm:

Step 1: Choose 'k' random feature vectors as initial centroids c1, c2, ..ck of K clusters.
Step 2: Calculate the distance of the data point Fi to the centroid cj of every cluster.
Step 3: update old clusters with the help of data points Fi belonging to the same cluster.
Step 4: Let dij be the distance from feature vector Fi to the cluster cj.
Step 5: Find out the nearest centroid for the data point Fi. Let it be cj. Thus dij is the smallest distance from all the centroids to the feature vector Fi.
Step 6: Check whether any other centroid is also reasonably nearer to the data point Fi. For this divide all the similarity distances from Fi to all the clusters with dij. That is S = k: dik/dij <= threshold and i != j
Step 7: If S = Ø, then Fi belongs to the lower and upper approximations of cj.
Step 8: Else Fi belongs to the upper approximation of cj and upper approximation of ck, for every k belonging to S.
Step 9: Calculate new centroids c1 to ck using equations 4, 5, 6 and 7.
step 10: Calculate the distance of the data point Fi to every cluster cj.
Step 11: update new clusters with the help of data points Fi belonging to the same cluster.
Step 12: Repeat from step 3 to step 11 until new clusters - old clusters = 0.0001.
Step 13: Stop.

IV. IMAGE CLASSIFICATION

After clustering the image pixels with the help of rough sets, pixels of the same cluster are allotted the same colour and later are displayed in the form of an image to get the classified image.

V. EXPERIMENTAL SETUP

Algorithms are implemented on many Google Earth images of various regions as mentioned in data sets and few of them are presented here. All algorithms are implemented in Matlab and are applied on small images of various sizes cropped from the original Google Earth image. For every pixel of the Google Earth image, experiments are carried out on a neighbourhood window of 81 X 81 pixels, 51 X 51 pixels and on 31 X 31 pixels. Finally, a window of size 51 X 51 was empirically selected. Ground truths of the image are obtained by manually segmenting the image after observing a more closer picture from the Google Earth.

A. Data sets

1) Clipping of Amaravathi area from Andhra Pradesh state captured from Google Earth on 27-12-2018 with 80.2929994^o longitude, 16.61889^o latitude and 978 ft eye altitude.
2) Clipping of Tamilnadu area captured from Google Earth on 26-12-2017 with 78.492388^o longitude, 11.191777^o latitude and 1406 ft eye altitude.
3) Clipping of Kollipara area from Andhra Pradesh state captured from Google Earth on 19-10-2017 with 80.771357^o longitude, 16.284618^o latitude and 755 ft eye altitude.
4) Clipping of Kollipara area from Andhra Pradesh state captured from Google Earth on 20-10-2017 with 80.775660^o longitude, 16.283197^o latitude and 597 ft eye altitude.
5) Clipping of Nandyala area from Andhra Pradesh state captured from Google Earth on 19-10-2017 with 78.6575^o longitude, 15.57278^o latitude and 7251 ft eye altitude.
6) Clipping of Pedavadlapudi area from Andhra Pradesh state captured from Google Earth on 16-10-2017 with 80.622495^o longitude, 16.413325^o latitude and 878 ft eye altitude.

VI. RESULTS AND DISCUSSIONS

A. Rough sets with intensity values

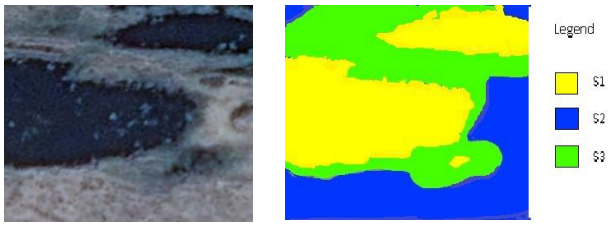

(a) (b)

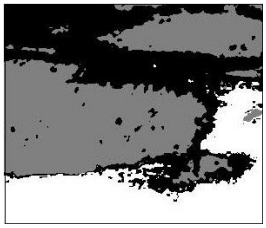

(c)

Fig. 4. Amaravathi clip: Classification results for rough sets with intensity values (a) Original image (b) Ground truth image and (c) Classified image for rough sets with intensity values

Experiments are conducted on various images to classify them with the help of rough sets based on the individual radiometric values of the pixel [1]. For some images like figure 4, where every segment has a specific and solid gray value, the results are good. For example in figure 4, figure 4a shows the original clip of Amaravathi region, figure 4b shows the ground truth image and figure 4c shows the final classified image, classified using individual radiometric values and rough sets. It is clearly evident that the final classification of this image is very much nearer to the ground truth.

But if the image such as figure 5 is considered, the final classified image figure 5c do not agree with the ground truth. This Figure contains two colors black and white which should represent two different segments. But, the second segment also contains much of the black color resulting which, this image was unable to classify the given image into two types of crops. Figure 5 is of Tamilnadu region. Figure 5a is the original true color image, 5b is the ground truth image and finally figure 5c is the classified image, using the radiometric values and rough sets.

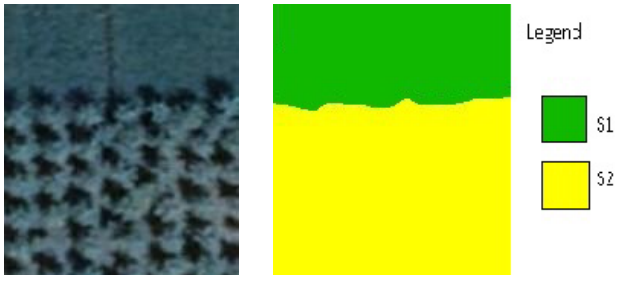

(a) (b)

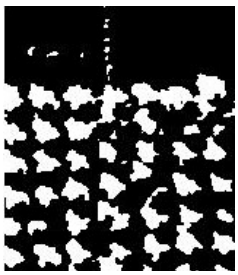

(c)

Fig. 5: Tamilnadu clip: Classification results for rough sets with intensity values (a) Original image (b) Ground truth image and (c) Classified image for rough sets with intensity values

B. GLCM and Rough Sets

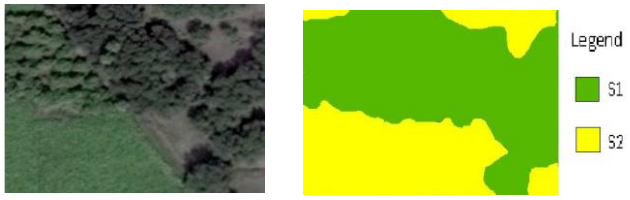

(a) (b)

(c)

Fig. 6: kollipara clip2: Classification results for rough sets with GLCM (a) Original image (b) Ground truth image and (c) Classified image for rough sets and GLCM

For most of the images, features extracted using GLCM have not converged with the help of rough sets. Features calculated with GLCM could be classified with the help of some training data which was already known. Even though converged with the help of rough sets, it yielded poor results. For example, figure 6 shows the Google Earth image of Kollipara region of Andhra Pradesh, India. Figure 6a is the original image, figure 6b presents the ground truth image and figure 6c presents the classified image using the features extracted from GLCM and clustered with the help of rough sets. From this figure, it is clearly evident that the GLCM + rough sets algorithm has not given the desired result.

C. LCD and Rough Sets

(a) (b)

(c)

Fig. 7: nandyala clip: Classification results for rough sets with Linear contact distributions (a) Original image (b)Ground truth image and (c) Classified image for rough sets and Linear contact distributions.

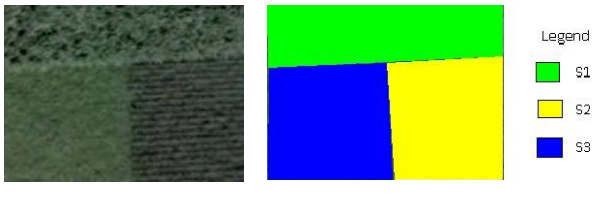

(a) (b)

(c)

Fig. 8: kollipara clip3: Classification results for rough sets with Linear contact distributions (a) Original image (b)Ground truth image (c) Classified image for rough sets and Linear contact distributions.

Experiments are carried out to cluster the features calculated using LCD [11] as per equation 1 and rough sets. For figures like figure 7, experiments yielded good results.

Retrieval Number: B2822078219/19©BEIESP
DOI:10.35940/ijrte.B2822.098319
Journal Website: www.ijrte.org

Published By:
Blue Eyes Intelligence Engineering
& Sciences Publication

For example, figure 7a is a Google Earth true color image of Nandyala region.
Figure 7b shows the ground truth image and figure 7c presents the resultant classified image with LCD and Rough Sets. It can be seen that resultant image is very much nearer to the ground truth and the said algorithm was able to classify the image as thick forest and sparse forest regions. But, for figures like figure 8 and figure 9, LCD + Rough sets did not yield satisfying results. Figure 8 is the image of Kollipara region and figure 9 is the image of Pedavadlapudi region. If the final classified images and respective ground truths are observed, it can easily be found that the results are not very much satisfying.

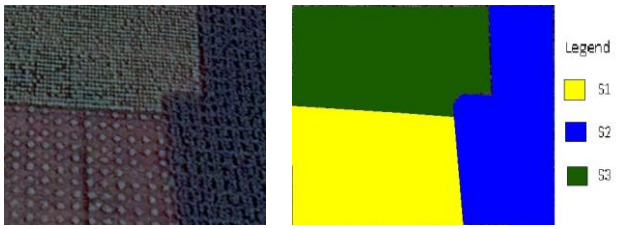

(a) (b)

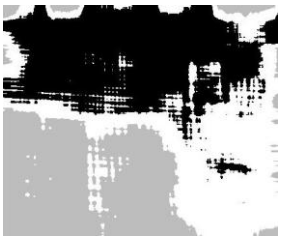

(c)

Fig. 9: Pedavadlapudi clip: Classification results for rough sets with Linear contact distributions (a) Original image (b) Ground truth image and (c) Classified image for rough sets and Linear contact distributions.

D. RTBFCA (LCD + FOS and Rough sets)

Experiments have been conducted to classify the image with the help of newly proposed algorithm RTBFCA. In this algorithm, LCD and FOS are used for texture feature extraction and are clustered with the help of rough sets. Figures 10, 11, 12, 13, 14, 16, and 17 present that the final segmented images are very much nearer to their ground truth images. RTBFCA provides good classification results for almost all images.

E. Quantitative analysis

In order to give some insights into the numerical accuracy of the results obtained, the resultant images of the algorithms are compared quantitatively with the ground truth images with the help of various performance measures like Dice coefficient, Jaccard coefficient, Precision and segmentation accuracy [8], [13]. If final classified image is represented with 'X' and the ground truth image is represented by 'Y', then the formula of Dice coefficient is given by

$$\text{Dice coefficient} = \frac{2*(X \bigcap Y)}{|X|+|Y|} \qquad (8)$$

As per the literature, the Dice coefficient value ranges between 0 and 1. The result is said to be poor if the dice coefficient value tends towards 0 and high when the Dice coefficient value tends towards 1.

Zijdenbose et al [41] propose that the segmentation is good if the Dice coefficient value is greater than 0.700. Similarly, Jaccard coefficient is given by

$$\text{Jaccard coefficient} = \frac{X \bigcap Y}{X \bigcup Y} \qquad (9)$$

Tables I and II show the performance results of various images with the algorithms "Intensity values + rough sets", "GLCM + rough sets", "LCD + rough sets" and finally the proposed algorithm RTBFCA (LCD + FOS + rough sets). Both the tables clearly show that for figure 4, the results of "intensity values + Rough sets" are close to our proposed algorithm. In all other cases, it is clearly evident that the proposed algorithm performs very much better than the "Intensity values + Rough Sets" algorithm. When compared with "GLCM + rough sets", the proposed algorithm performs outstandingly as the features did not even converge for few images and for remaining images RTBFCA does better. Also, the proposed algorithm performed well when compared to "LCD + Rough sets".
Precision and Segmentation accuracy are other performance evaluation measures which are used to identify the similarity between the segmentation result and the ground truth image [10], [30], [13]. To calculate the Precision or Segmentation accuracy, four parameters TP, TN, FP and FN are calculated.
1. True positive (TP): Number of true pixels in the ground truth correctly identified as segmented pixels.
2. True negative (TN): Number of false pixels in the ground truth correctly identified as segmented pixels.
3. False positive (FP): Number of true pixels in the ground truth wrongly identified in the segmentation result.
4. False negative (FN): Number of false pixels in the ground truth wrongly identified in the segmentation result.
Precision is the positive predictive value and segmentation accuracy is the fraction of the total sample that is correctly identified. Precision and segmentation accuracy are calculated as

$$\text{Precision} = \frac{TP}{TP+FP} \qquad (10)$$

$$\text{Segmentation Accuracy} = \frac{TP+TN}{TP+TN+FP+FN} \qquad (11)$$

Tables III and IV, present that the proposed algorithm performed better than its counterparts.

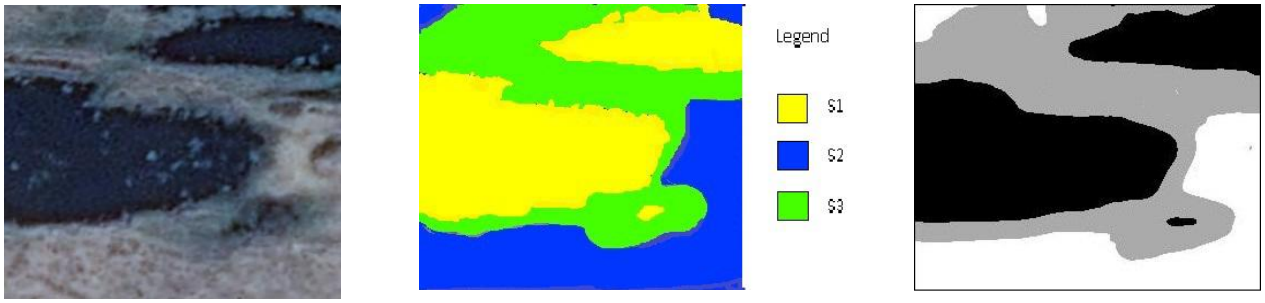

(a) (b) (c)

Fig. 10: Amaravathi clip: Classification results for RTBFCA (a) Original image (b) Ground truth image (c) Classified image for RTBFCA

(a) (b) (c)

Fig. 11: Nandyala clip: Classification results for RTBFCA (a) Original image (b) Ground truth image (c) Classified image for RTBFCA

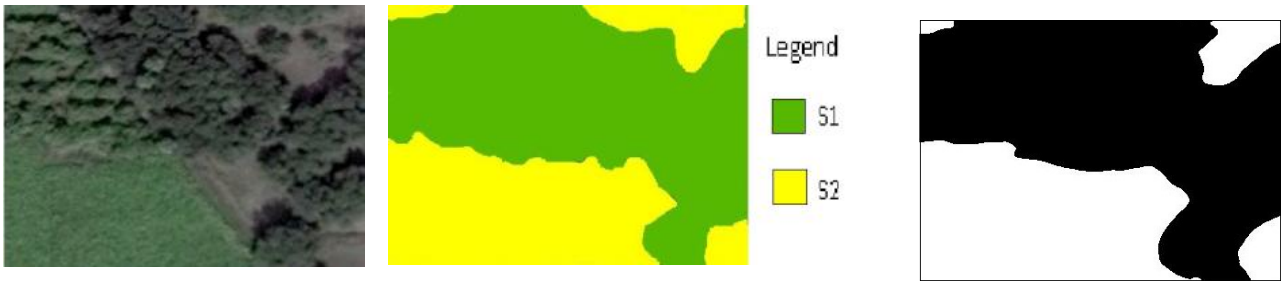

(a) (b) (c)

Fig. 12: Kollipara clip2: Classification results for RTBFCA (a) Original image (b) Ground truth image (c) Classified image for RTBFCA

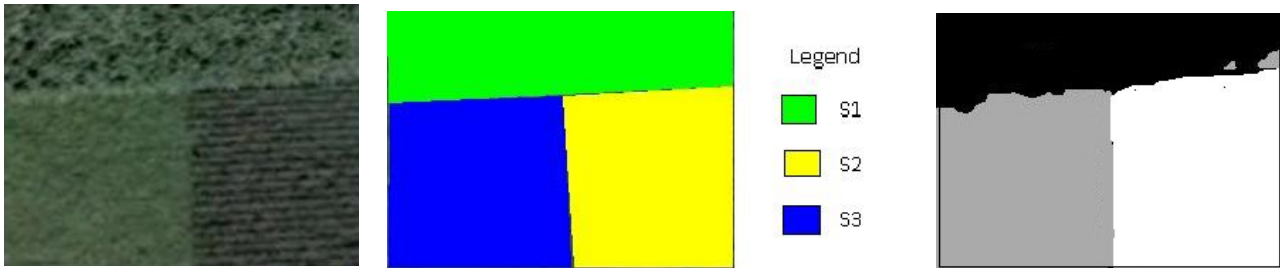

(a) (b) (c)

Fig. 13. Kollipara clip3: Classification results for RTBFCA (a) Original image (b) Ground truth image (c) Classified image for RTBFCA

Retrieval Number: B2822078219/19©BEIESP
DOI:10.35940/ijrte.B2822.098319
Journal Website: www.ijrte.org

Published By:
Blue Eyes Intelligence Engineering
& Sciences Publication

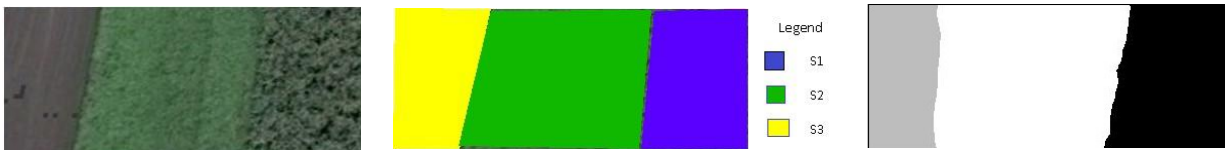

(a) (b) (c)

Fig. 14: Kollipara clip1: Classification results for RTBFCA (a) Original image (b) Ground truth image (c) Classified image for RTBFCA

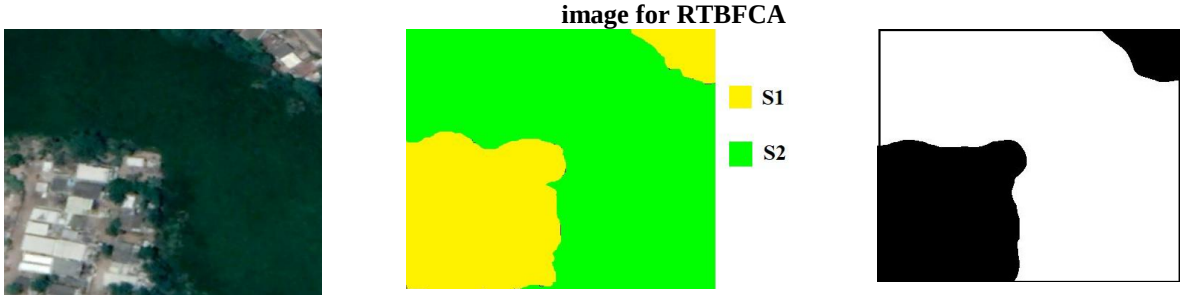

(a) (b) (c)

Fig. 15: Guntur clip: Classification results for RTBFCA (a) Original image (b) Ground truth image (c) Classified image for RTBFCA

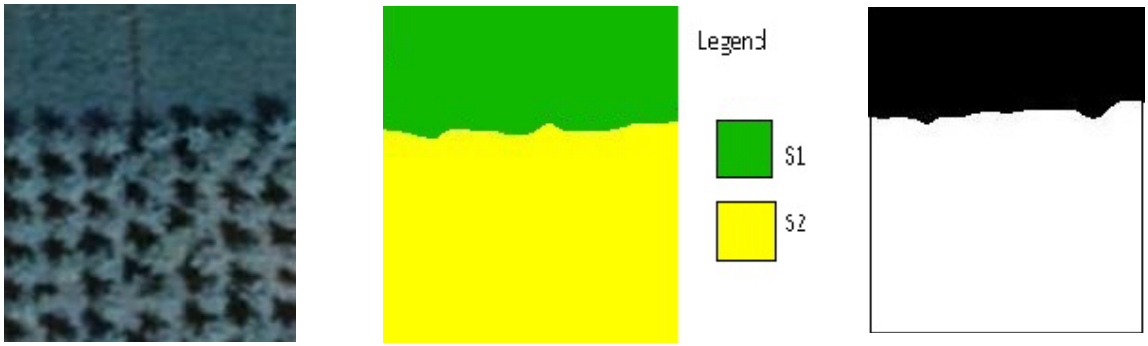

(a) (b) (c)

Fig. 16: Tamilnadu clip: Classification results for RTBFCA (a) Original image (b) Ground truth image (c) Classified image for RTBFCA

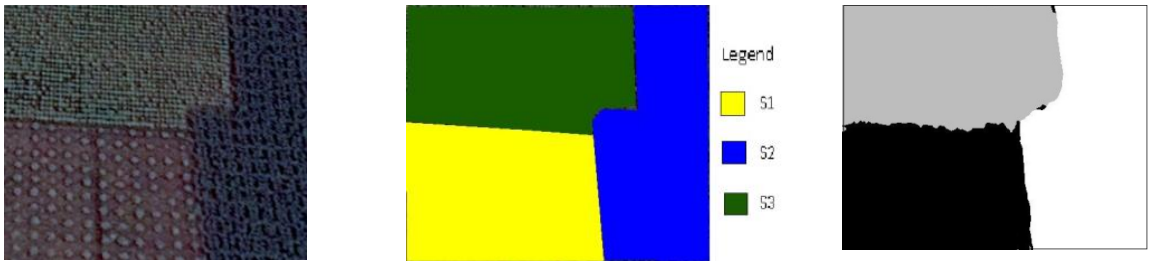

(a) (b) (c)

Fig. 17: pedavadlapudiclip: Classification results for RTBFCA (a) Original image (b) Ground truth image (c) Classified image for RTBFCA

Table I. Dice Coefficient

S.No	Image	Segment	Intensity values + Rough sets	GLCM + Rough sets	LCD + Rough sets	RTBFCA
1	Amaravathi clip	S1	0.944	Not converged	0.607	0.945
		S2	0.938		0.077	0.932
		S3	0.881		0.443	0.872
2	Kollipara clip1	S1	0.618	Not converged	0.599	0.979
		S2	0.901		0.000	0.954
		S3	0.981		0.594	0.984
3	Kollipara clip2	S1	0.725	0.620	0.566	0.918
		S2	0.662	0.359	0.000	0.936
4	Kollipara clip3	S1	0.979	Not converged	0.817	0.950
		S2	0.858		0.904	0.974
		S3	0.966		0.586	0.986
5	Nandyala clip	S1	0.948	0.878	0.889	0.979
		S2	0.847	0.000	0.059	0.875
6	Pedavadlapudi clip	S1	0.804	0.000	0.713	0.869
		S2	0.610	0.207	0.679	0.911
		S3	0.586	0.007	0.860	0.906
7	Tamilnadu clip	S1	0.599	Not converged	0.649	0.985
		S2	0.834		0.838	0.972
8	Guntur clip	S1	0.961	Not converged	0.825	0.983
		S2	0.968		0.527	0.975

TABLE II. Jaccard coefficient

S.No	Image	Segment	Intensity values + Rough sets	GLCM + Rough sets	LCD + Rough sets	RTBFCA
1	Amaravathi clip	S1	0.782	Not converged	0.407	0.846
		S2	0.767		0.037	0.764
		S3	0.611		0.233	0.674
2	Kollipara clip1	S1	0.439	Not converged	0.341	0.937
		S2	0.756		0.000	0.875
		S3	0.956		0.274	0.903
3	Kollipara clip2	S1	0.558	0.438	0.385	0.808
		S2	0.487	0.199	0.000	0.855
4	Kollipara clip3	S1	0.868	Not converged	0.603	0.915
		S2	0.508		0.697	0.751
		S3	0.732		0.373	0.934
5	Nandyala clip	S1	0.899	0.761	0.742	0.939
		S2	0.478	0.000	0.027	0.740
6	Pedavadlapudi clip	S1	0.970	0.000	0.924	0.986
		S2	0.929	0.427	0.905	0.973
		S3	0.883	0.020	0.966	0.970
7	Tamilnadu clip	S1	0.361	Not converged	0.397	0.940
		S2	0.499		0.704	0.932
8	Guntur clip	S1	0.858	Not converged	0.657	0.953
		S2	0.906		0.522	0.928

Table III. Precision table

S.No	Image	Segment	Intensity values + Rough sets	GLCM + Rough sets	LCD + Rough sets	RTBFCA
1	Amaravathi clip	S1	0.813	Not converged	0.409	0.913
		S2	0.837		0.431	0.874
		S3	0.649		0.615	0.701
2	Kollipara clip1	S1	0.826	Not converged	0.924	0.937
		S2	0.793		0.000	0.884

		S3	0.988		0.274	0.974
3	Kollipara clip2	S1	0.574	0.438	0.390	0.883
		S2	0.923	0.995	0.000	0.877
4	Kollipara clip3	S1	0.913	Not converged	0.611	0.787
		S2	0.542		0.716	0.560
		S3	0.750		0.926	0.941
5	Nandyala clip	S1	0.483	0.780	0.779	0.998
		S2	0.746	0.000	0.130	0.740
6	Pedavadlapudi clip	S1	0.827	0.000	0.770	0.905
		S2	0.693	0.180	0.676	0.707
		S3	0.621	0.150	0.923	0.940
7	Tamilnadu clip	S1	0.369	Not converged	0.930	0.996
		S2	0.807		0.704	0.932
8	Guntur clip	S1	0.906	Not converged	0.677	0.955
		S2	0.992		0.432	0.990

Table IV. Segmentation accuracy table

.No	Image	Segment	Intensity values + Rough sets	GLCM + Rough sets	LCD + Rough sets	RTBFCA
1	Amaravathi clip	S1	0.742	Not converged	0.499	0.779
		S2	0.801		0.708	0.811
		S3	0.731		0.713	0.757
2	Kollipara clip1	S1	0.807	Not converged	0.624	0.894
		S2	0.787		0.721	0.694
		S3	0.983		0.441	0.894
3	Kollipara clip2	S1	0.693	0.510	0.438	0.706
		S2	0.692	0.510	0.405	0.768
4	Kollipara clip3	S1	0.772	Not converged	0.738	0.825
		S2	0.676		0.696	0.754
		S3	0.673		0.702	0.845
5	Nandyala clip	S1	0.716	0.634	0.580	0.728
		S2	0.650	0.758	0.766	0.849
6	Pedavadlapudi clip	S1	0.763	0.628	0.767	0.812
		S2	0.690	0.337	0.714	0.784
		S3	0.723	0.599	0.827	0.896
7	Tamilnadu clip	S1	0.513	Not converged	0.741	0.824
		S2	0.505		0.684	0.711
8	Guntur clip	S1	0.769	Not converged	0.651	0.783
		S2	0.843		0.593	0.875

VII. CONCLUSION

Extracting texture features with the help of LCD and clustering with the help of rough sets to classify a remote sensing image is studied in this paper. A new algorithm RTBFCA has been proposed. It has been compared with various other algorithms like Intensity values + rough sets algorithm, GLCM + rough sets algorithm and with LCD + rough sets algorithm. Each of these algorithms are good at classifying some kinds of images but failed to classify some other types of images. RTBFCA, where texture features are extracted with LCD + FOS and are clustered with the help of rough sets performed well for almost all images. The subjective analysis shows that RTBFCA performed betterthan its counterparts and is able to classify buildings, forests, crops, water, etc from land cover remote sensing images.
It was also able to classify different crops with close patterns and are also of same colour. When analyzed with quantitative performance measures like Dice coefficient, Jaccard coefficient, segmentation accuracy, and precision, the proposed algorithm RTBFCA performed fairly well. Dice coefficient values of all the images presented are greater than 0.85 and for most of them, it is greater than 0.90. Segmentation accuracy values of all segments for RTBFCA algorithm is greater than 0.75 and for most of them, it is greater than 0.80. This proves the efficiency of the algorithm. Hence both from subjective and objective analyses, it could be said that RTBFCA definitely performed well when compared to its counterparts.

ACKNOWLEDGEMENT

The authors wish to thank Google Earth, for providing the satellite images and UGC (University Grants Commission). This work was supported by a minor research project grant from UGC.

REFERENCES

1. N Anupama, S Srinivas Kumar, and E sreenivas Reddy. Rough set based MRI medical image segmentation using optimized initial centroids. International journal of emerging technologies in computational and applied sciences, 13:90–98, 2013.
2. N Anupama, S Srinivas Kumar, and E sreenivas Reddy. Generalizedrough intuitionistic fuzzy c-means for MRI brain image segmentation. IET image processing, 11(9):777–785, September 2017.
3. S. Arivazhagan and L. Ganesan. Texture segmentation using wavelet transform. Pattern Recognition Letters, 24(16):3197–3203, December 2003.
4. A.V.Kavitha, A.Srikrishna, and Ch.Satyanarayana. Unsupervised linear contact distributions segmentation algorithm for land cover high-resolution panchromatic images. Multimedia tools and applications, pages 1–19, 2018.
5. A.V.Kavitha, A.Srikrishna, and Ch.Satyanarayana. An efficient texture feature extraction algorithm for high resolution land cover remote sensing image classification. International Journal of Image, Graphics and Signal Processing, 10:21–28, December 2018.
6. J.A. Benediktsson and Pesaresi. Classification and feature extraction for remote sensing images from urban areas based on morphological transformations. IEEE Trans. on Geoscience and remote sensing, 41(9):1942–1949, 2003.
7. D.A. Clausi and Huang Deng. Design-based texture feature fusion using Gabor filters and co-occurrence probabilities. IEEE Trans on image processing, 14(7):925–936, June 2005.
8. L.R. Dice. Measures of the amount of ecologic association between species. Ecology, 26:297–302, July 1945.
9. P.C. Doraiswamy and et al. Crop classification in the U.S. corn belt using modis imagery. IEEE Proceedings of Geoscience and Remote Sensing Symp, 45(4):1074 – 1083, 2007.
10. Richard O. Duda and E. Hart Peter. Pattern classification and scene analysis. Wiley, New York, 3 edition, 1973.
11. I. Epifanio and P Soille. Morphological texture features for unsupervised and supervised segmentation of natural landscapes. IEEE Trans on Geoscience and Remote sensing, 45(4):1074 – 1083, 2007.
12. Irene Epifanio and Guillermo Ayala. A random set view of texture classification. IEEE trans of image processing, 11(8):859–867, August 2002.
13. J.L. Fleiss. The measurement of interrater agreement. In: Statistical methods for rates and proportions. John Wiley and Sons, New York, 2 edition, 1981.
14. L. Ghouti, A. Bouridane, M.K. Ibrahim, and S. Boussakta. Digital image watermarking using balanced multiwavelets. IEEE Trans on Signal Processing, 54(4):1519–1536, 2006.
15. Guang-Jun, DongYong-Sheng, and ZhangYong-Hong Fan. Remote sensing image classification algorithm based on rough set theory. Advances in soft computing, 40:1–9, October 2007.
16. H. Hagner, O.and Reese. A method for calibrated maximum likelihood classification of forest types. Remote sensing of environment,110:438–444, 2007.
17. R.M. Harlick, K. Shanmugam, and I. Dinstein. Texture features for image classification. IEEE Trans on Systems, Man. and Cybernetics, SMC-3:610–621, November 1973.
18. L. Jianzhuang and et al. Wenqing, L. Automatic thresholding of gray level pictures using two-dimensional Otsu method. IEEE proc on Circuits and systems, 1991.
19. Sascha Klemenjak, Bj¨orn Waske, Silvia Valero, and Jocelyn Chanussot. Automatic detection of rivers in high-resolution SAR data. IEEE Journal of selected topics in applied earth observations and remote sensing, 5(2):1–9, October 2012.
20. Deren Li, Guofeng Zhang, Zhaocong Wu, and Lina Yi. An edge embedded marker-based watershed algorithm for high spatial resolution remote sensing image segmentation. IEEE Trans on image processing, 19(10):2781 – 2787, May 2010.
21. Lingras, Pawan, and Chad West. Interval set clustering of web users with rough k-means. Journal of intelligent information systems, 23(1):5–16, 2004.
22. C. Luc and L. Sebastien. Road network extraction from remote sensing using region-based mathematical morphology. IEEE procs. on Pattern recognition in remote sensing, 2014.
23. Mauro Dalla Mura, Jon Atli Benediktsson, and et al. Morphological attribute profiles for the analysis of very high-resolution images. IEEE Trans on geoscience and remote sensing, 48(10):3747–3762, October 2010.
24. Rudra Kalyan Nayak, Debahuti Mishra, Kailash Shaw, and Sashikala Mishra. Rough set based attribute clustering for sample classification of gene expression data. International conference on Modelling optimization and Computing, 38:1788–1792, December 2012.
25. N. OTSU. A threshold selection method from the gray level histogram.IEEE Trans. on Systems, Man, and Cybernetics, 9(1):62–66, 1979.
26. P.Mohanaiyah, P.satyanarayana, and L.GuruKumar. Image texture feature extraction using glcm approach. International journal of scientific and research publications, 3(5), May 2013.
27. Andrik Rampun, Harik strange, and et al. Texture segmentation using different orientations of glcm features. 6th International Conference on Computer Vision / Computer Graphics Collaboration Techniques and Applications, MIRAGE, June 2013.
28. N. Robbe and T. Hengstermann. Remote sensing of marine oil spills from airborne platforms using multi-sensor systems. WIT trans on Ecology and the environment, 2006.
29. M. Schroder and A. Dimai. Texture information in remote sensing images-a case study. Proc of WTA., 1998.
30. Warfield Simon, K. Kelly, H.Zou, and M. William Wells. Simultaneous truth and performance level estimation (staple)- an algorithm for the validation of image segmentation. IEEE Trans on medical imaging, pages 903–921, July 2004.
31. Benqin Song, Jun Li, and et al. Remotely sensed image classification using sparse representations of morphological attribute profiles. IEEE Trans on geoscience and remote sensing, 52(8):5123–5136, August 2014.
32. G. N. Srinivasan and G. Shobha. Statistical texture analysis. Proceedings of world academy of science, engineering and technology, 36:1264–1269, December 2008.
33. Safaa Muthana Sulaiman and N. Anupama. Texture and Gabor wavelet-based classification of hysteroscopy images of the endometrium. International journal of engineering science and computing, 7(5):12138–12142, May 2017.
34. Ying Sun and Guo jin He. Segmentation of high-resolution remote sensing image based on marker-based watershed algorithm. IEEE conf procs at Shandong, China, October 2008.
35. Ying Wang, Xiaoyun Liu, Zhensong Wang, and Wufan Chen. Multispectral remote sensing image classification algorithm based on rough set theory. IEEE International Conference on Systems, Man and Cybernetics, October 2009.
36. Zhaocong Wu. Research on remote sensing image classification using neural network based on rough sets. International Conferences on Info-Tech and Info-Net. Proceedings, November 2001.
37. L. Xue, X. Yang, and et al. Building extraction of SAR images using morphological attribute profiles. Springer Communications signal processing and systems, 202:13–21, 2012.
38. Pawlak Z. Rough sets: Theoretical aspects of reasoning about data. Kluwer, The Netherlands, 1991.
39. Jian Zhao and Xin Pan. Remote sensing image feature selection based on rough set theory and multi-agent system. 12th International Conference on Fuzzy Systems and Knowledge Discovery, June 2015.
40. Wu Zhaocong and Li Deren. Neural network based on rough sets and its application to remote sensing image classification. Geospatial information science, 5(2):17–21, June 2002.
41. A. P. Zijdenbos, B. M. Dawant, R.A. Margolin, and A. C. Palmer. Morphometric analysis of white matter lesions in mr images: method and validation. IEEE Trans Med Imaging, 13:716–724, 1994.

AUTHORS PROFILE

Smt. A.V. Kavitha is working as an Associate professor and Head of the Department of Computer science at Sri. A.B.R. Government degree college, Repalle, Guntur (Dt), Andhra Pradesh, India and is a research scholar at Jawaharlal Nehru Technological University, Kakinada, Andhra Pradesh, India. She is having 23 years of teaching experience and six years of research experience. She has published 16 papers in various national and international journals and conferences. Her research interests are in Image processing, Pattern recognition, Remote sensing, and computer vision.

Dr. A. Srikrishna is professor and head of the Department of Information and Technology at RVR & JC College of engineering, Chowdavaram, Guntur, Andhra Pradesh, India. She has 27 years of teaching experience. She has published more than 35 papers in international journals and conferences. She has received major and minor research project grants from UGC and AICTE. She has authored a book entitled "Parametric Based Morphological Transformation for Contrast Enhancement. Her research interests are in Image processing, Computer vision, Information security, and algorithms.

Dr. Ch. Satyanarayana is a professor in Computer science and Engineering department, and director for Academic and Planning at Jawaharlal Nehru Technological University, Kakinada, Andhra Pradesh, India. He has guided 15 students for Ph.D. in Computer science and engineering. He is a senior member in IEEE and has published more than 150 papers in international journals and conferences. His research interests are in Image processing, Speech recognition and Pattern recognition and have eighteen years of experience.